Astron. Astrophys. 329, 147–154 (1998)

ASTRONOMY AND ASTROPHYSICS

Analysis of the irregular pulsations of AC Herculis

Z. Kolláth[2,1], **J.R. Buchler**[1], **T. Serre**[3], **and J. Mattei**[4]

[1] Physics Department, University of Florida, Gainesville, FL 32611, USA (buchler@phys.ufl.edu)
[2] Konkoly Observatory, Budapest, Hungary (kollath@buda.konkoly.hu)
[3] Observatoire de Paris, Meudon, France
[4] AAVSO, Cambridge, MA 02138, USA

Received 13 June 1997 / Accepted 12 August 1997

Abstract. The AAVSO lightcurve data of the irregularly pulsating star AC Herculis of the RV Tau class are analysed. The lightcurve is shown not to be compatible with a periodic, or even multiperiodic pulsation, even if allowance is made for evolution. Instead the best explanation is that the irregularly alternating cycles are a manifestation of low dimensional chaos. Our flow reconstruction suggests that the dynamics can be successfully embedded in 3 dimensions. Further, the (Lyapunov) fractal dimension of the underlying dynamic attractor is computed to be $2.05 \lesssim d_L \lesssim 2.45$, independent of the dimension of the reconstruction space. It is smaller than the value of $d_L \approx 3.1$ found for the more irregular lightcurve of R Sct. From these results we are led to conclude that the lightcurve is likely to have been generated by a 3 dimensional dynamics, i.e. by 3 first order ODEs. In simpler language, it expresses the remarkable fact that the observational value at any time $s(t_n)$ is a unique function h of the values at only three preceding observations, viz. $s(t_{n+1}) = h\big(s(t_n), s(t_{n-1}), s(t_{n-2})\big)$.

Key words: stars: individual: AC Her – stars: oscillations – methods: data analysis – methods: numerical – chaos

1. Introduction

In this paper we analyze the AAVSO data set of the lightcurve of AC Herculis that shows irregular pulsations with large cycle to cycle alternations in the lightcurve. The paper is organized in parallel to the analysis of R Scuti (Buchler, Serre, Kolláth & Mattei 1995 hereafter BSKM, Buchler, Kolláth, Serre & Mattei 1996, hereafter BKSM). Despite their membership in the same RV Tau class the lightcurves of these two stars are quite different. AC Her has a cycle time of 35 days, about half that of R Sct, has a much lower pulsation amplitude, and is much less irregular. From a practical point of view, the available AAVSO data set is shorter, there are more gaps and fewer points per cycle, and the relative noise level is higher, all of which make the analysis somewhat harder.

In Sect. 2 we show on the basis of Fourier spectral analysis and theoretical considerations that the pulsations are not compatible with periodic or multiperiodic behavior, even when evolution is allowed for. The pulsations must therefore be either of a chaotic or of a stochastic nature. (We follow the general trend of distinguishing the two by calling chaotic an erratic signal that is generated by a deterministic low dimensional dynamics whose form can be found, at least in principle, and stochastic a very high dimensional dynamics that is too complicated to be characterized otherwise than stochastically.) In Sect. 3 we perform a nonlinear analysis that shows that the observational data are indeed compatible with low dimensional chaos, and we determine its quantitative properties. This is followed by a discussion in Sect. 4, and we conclude in Sect. 5.

2. Standard analysis

For a description of the AAVSO observational data archive we refer to Percy and Mattei (1993). The data set of visual observations spans JD2437596 – 2449442. For most of our nonlinear analyses we use only the second part (after JD2445000) of the data where the coverage is better. The average (rms) error of the data is quite large, about 0.15 mag. However, the errors are found to have a Gaussian distribution, *independent of magnitude*, but not of luminosity, which is a reflection of the visual nature of the observations. This feature of the magnitudes is quite apparent in Fig. 1 where we have superposed the histograms for the errors for the data spit into three groups, viz. below, in and above the range 7.5 – 7.8 mag. Just as for R Sct we therefore analyze the magnitude rather than the more physical luminosity. We believe that thanks to the Gaussian error distribution we are able to extract a relatively good average signal from the bare data in the next section.

In Fig. 2a, on top, we display the *amplitude* Fourier spectrum (FS) of the averaged AAVSO data for the observed AC Her lightcurve. The spectrum is clearly dominated by four peaks. The lowest frequency peak is located at f_0=0.01326 d^{-1} (P_0=75.43 d). In the bottom row we show the spectral window

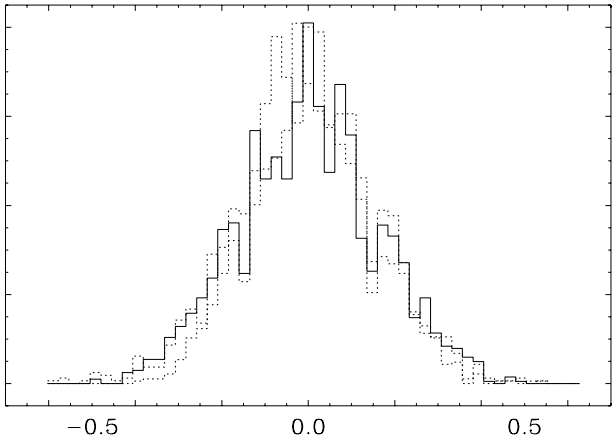

Fig. 1. Error distributions of the AAVSO data; data grouped into 3 ranges, below, in and above 7.5 to 7.8 mag.

which introduces some of the side-lobe structure that is evident in the top figure.

Prima facie the FS of AC Her seems to suggest periodicity (as does the lack of phase jumps in the pulsations, cf. Fig. 5 below). Therefore, in the second row we show the FS of the lightcurve with a periodic prewhitening with f_0 and its lowest 7 harmonics. (Actually the last, highest four harmonics improve the prewhitening very little). The phases of the three dominant harmonics, Φ_k, k=1, 3 vary in concordance with Φ_0 over the time span of the data (see Fig. 3 where we show Φ_0 and Φ_1). This establishes a strong harmonic or perhaps resonant connection among the four dominant peaks. However, the 'grass' in the FS is very high, and furthermore the lightcurve has several observationally well established local features that a periodic fit completely misses.

To investigate the possibly noisy origin of the left-over grass we take the periodic component (that has been used in the prewhitening of row 2 of Fig. 2b) and add simulated Gaussian observational noise, with an intensity as indicated by the AAVSO data, viz. ≈ 0.15 mag. The FS of a prewhitened realization of such a noisy periodic signal is shown in the bottom row of Fig. 2b. The grass of the prewhitened lightcurve FS (Fig. 2b top) is much larger than that of the simulated noisy periodic lightcurve (Fig. 2b bottom). (Note that the ordinate scales of Figs. 2a and 2b are different. For comparison the same, periodically prewhitened FS has therefore been shown in both figures.)

Could the pulsations be multiperiodic instead of periodic? To answer this question we first allow the eight dominant frequencies (i.e. f_0 and previously its harmonics) to be independent. This multiperiodic prewhitening (1) produces essentially no reduction in the grass of the FS compared to the periodic prewhitening, and (2) it does not improve the fit to the data. Next we perform a more extensive prewhitening using now f_0 and its 7 harmonics plus 24 *linearly independent* frequencies, chosen from the highest peaks in row 2 of Fig. 2a. The resultant FS is shown in the second row FS of Fig. 2b. Despite this large number of frequencies quite a bit of unresolved grass still remains in the FS that cannot be explained away as observational noise as a comparison with the last row indicates. In addition, an overlay of the 24–periodic fit on the AAVSO data shows that many significant features are still missed.

Furthermore one would be hard-pressed theoretically to explain the origin of 24 or more frequencies of oscillation in this star, particularly if the star is undergoing radial pulsations, as expected. Even if nonradial pulsations are involved and if these visual, necessarily whole disk, observations could resolve up to ℓ=2 modes, it would not be possible to account for all these 'observed' frequencies.

The lightcurve therefore *cannot reasonably be explained as being periodic or multiperiodic with constant frequencies*.

Could the star be undergoing noticeable evolution over the three decades that the data span? Fig. 3 reports the time-dependence of the phases Φ_0 and Φ_1 of the lightcurve for the frequencies f_0 and $f_1 = 2f_0$. Here we have used the whole 32.5 yr AAVSO dataset. Were one to interpret the phase variations as due to evolutionary changes in the frequency one might conclude from the two approximately parabolic arcs that the frequency changes linearly in time ($\dot{P}_0 = 4\times10^{-4}$), but that in addition there is a very strong frequency glitch around t=11 yr. However, one would be hard pressed to come up with a mechanism for such large glitches. Zsoldos (1988) claims to have found evidence for a periodic variation in the $O-C$ curve of the minima of AC her with a period of 9323 days on the basis of a much longer data set. We cannot check the existence of this modulation because of the shorter time span of the AAVSO data.

Very recently Percy et al. (1997) have studied the period changes of RV Tauri stars, including AC Her, with the Eddington-Plakidis test. They have concluded that the $O-C$ diagrams can be interpreted as a superposition of random errors in the measured times of minimum, and random cycle-to-cycle fluctuations in the period. This is very supportive of our interpretation of these pulsations as chaos.

If, despite the preceding discussion, one still insisted on interpreting the pulsations as multiperiodic, then one should observe a systematic change in all the frequencies and in the associated amplitudes. We have therefore partitioned the whole AAVSO data set into quarters. Except for f_0 and its three harmonics already considered there is no apparent systematic variation in the grass. Fig. 4 displays the FS of the successive partitions of the data, all prewhitened and scaled the same way as the whole data set that has been shown in the second row of Fig. 2b.

In order to offer an alternative explanation for the phase variations of AC Her, we also show in Fig. 3 the phase variations obtained from the magnitude variations of numerical hydrodynamic simulations of the pulsations of a W Vir model (Kovács & Buchler 1988, Buchler 1993, Gouesbet et al. 1997). Following the same reasoning as for AC Her one might interpret the phase variations again as indicating a linear time dependence of the frequency (increasing with time here), also with an abrupt frequency shift at 27 yr. However, here we are absolutely sure that such an interpretation would be incorrect! Indeed, there

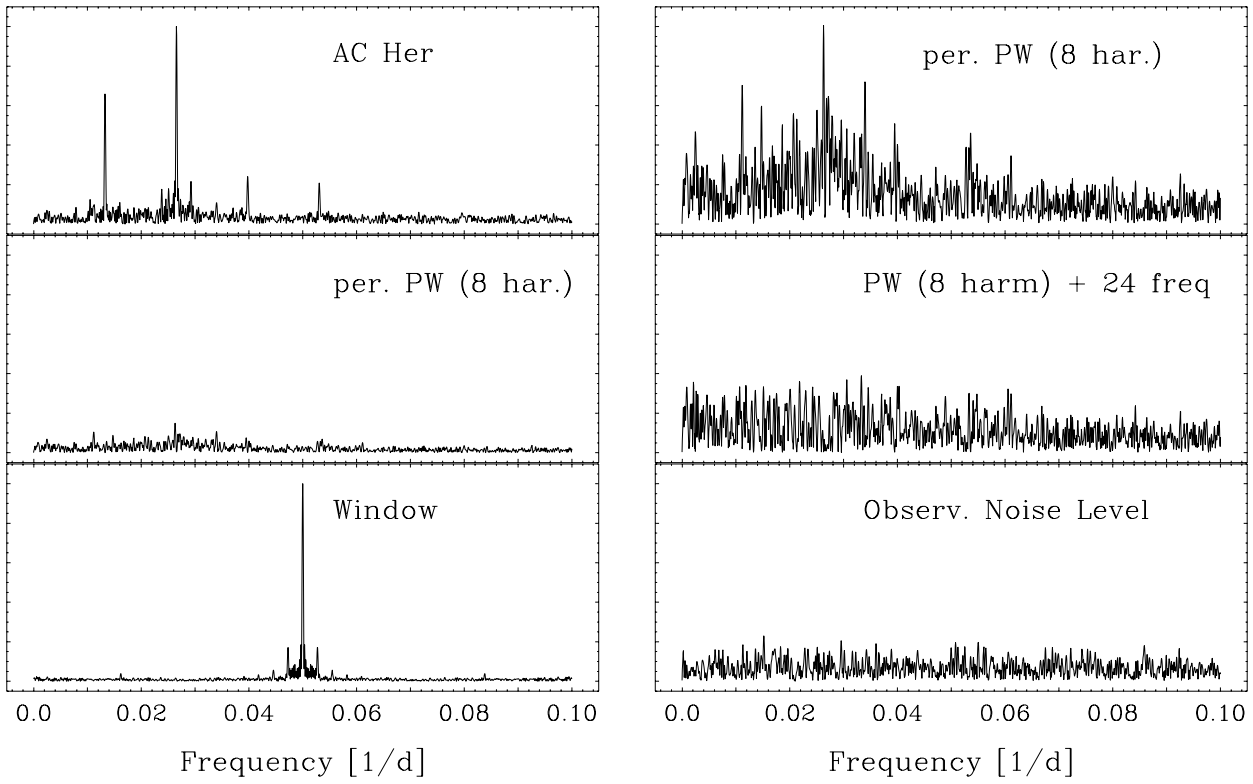

Fig. 2. a (left) Fourier Spectra. *Top row:* AAVSO data; *2nd row:* periodic prewhitening with f_0 and 7 harmonics; *3rd row:* spectral window; (all subfigures on same ordinate scale). **b** (right) Fourier Spectra; *Top row:* periodic prewhitening with f_0 and 7 harmonics; *2nd row:* multiperiodic prewhitening with f_0 and 7 harmonics plus the 23 most important independent frequencies; *bottom row:* expected observational noise level (cf. text); all three figures have the same ordinate scale.

is no evolution built into the W Vir model, and the pulsations have definitely been shown to be chaotic. The *phase variations are a natural result of the chaotic nature of the pulsations*, and *over short time-intervals they can give an erroneous impression of periodicity*. In accordance with our preceding discussion we therefore suggest that the apparent piecewise parabolic behavior in AC Her likewise is spurious and that the phase variations also have a chaotic origin.

We thus conclude that the pulsations of *AC Her cannot either be explained as those of an evolving multiperiodic star*.

The presence of spots also seems an unlikely explanation for the irregular pulsations of this type of luminous star. There is always the possibility of stochasticity, for example caused by internal convection. It is hard to rule out a nonlinear stochastic process. However, in the spirit of Occam's razor, if a simpler valid explanation can be found we see no need to search for a stochastic description which by its very nature would just push our ignorance further down the line.

We are thus led to investigate if the pulsations can be due to an underlying low dimensional chaotic dynamics. In a priori support of such an explanation we recall that the recent nonlinear analysis of the R Sct lightcurve as well as the modelling of W Vir models have indicated such chaotic behavior.

It might be rightly objected that these stars are likely to have turbulent motions, and that it is well known that turbulence is a *high* dimensional phenomenon. We have already addressed this issue in BKSM. For our approach to make sense the pulsation must be dominated by a large amplitude, low dimensional dynamics. The high dimensional, low amplitude turbulent jitter can then be filtered out, for example by our averaging and reconstruction. The success of our analysis seems to indicate that in the case of the pulsating stars of interest to us here, such a separation is indeed possible.

We now turn to the type of nonlinear analysis that can uncover low dimensional chaos when it is present in the data. (We refer a reader who is unfamiliar with chaos to the excellent reviews by Abarbanel et al. 1993 and Weigend & Gershenfeld 1994).

3. Global flow reconstruction

In a recent publication Serre, Kolláth & Buchler (1995, hereafter SKB; see also Buchler 1997 for a lecture note, or Gouesbet et al. 1997 for more general review) introduced a nonlinear time-series analysis, the global flow reconstruction method, that is suitable for astronomical data. A prior reading of these papers is suggested, not only for a description of the method but also for the notation and terminology that is used here. The application to the analysis of the lightcurve of R Sct appears in BSKM and BKSM.

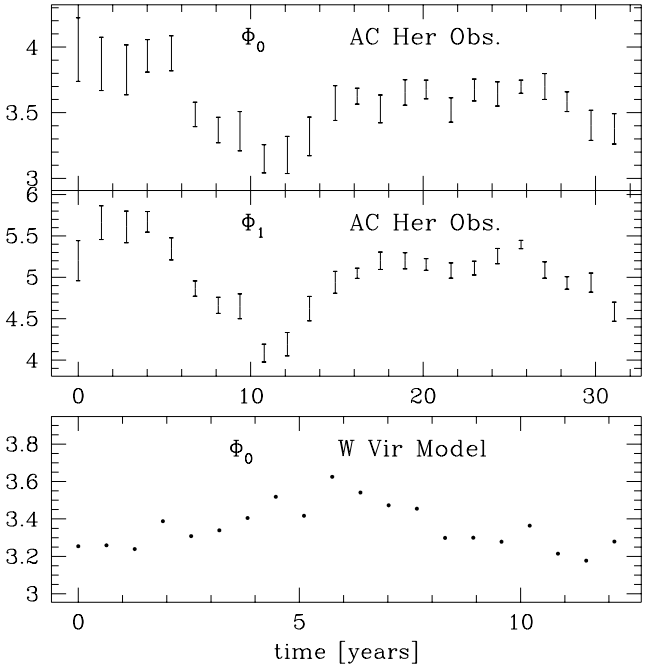

Fig. 3. *Top:* Time-dependence of the phases Φ_0 and Φ_1 over the span of the AC Her data set, *bottom:* Variation of the phase Φ_0 with time over the span of a corresponding data set of W Vir numerical model pulsations.

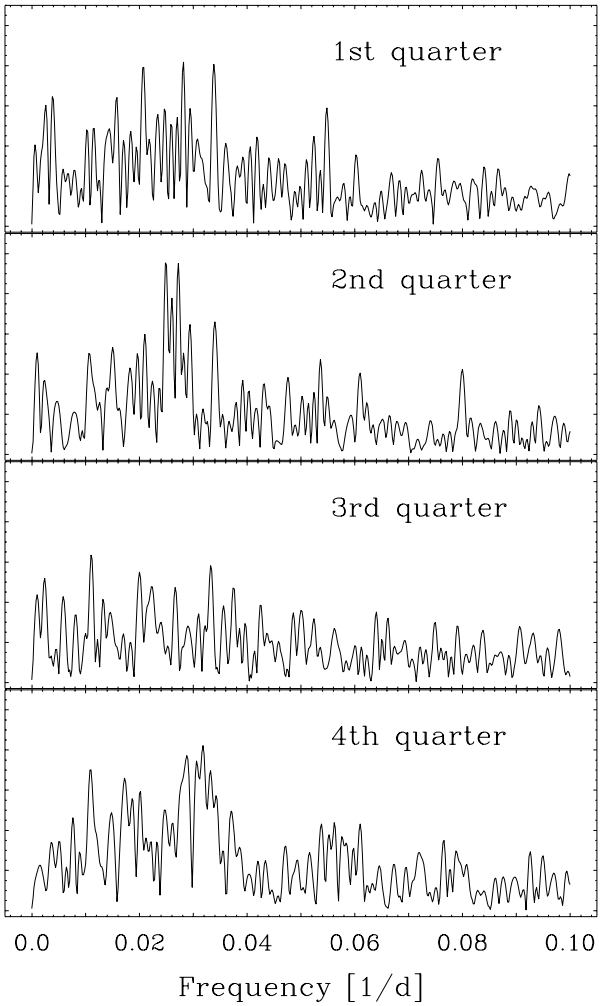

Fig. 4. Fourier Spectra of the prewhitened successive quarter partitions of the AAVSO data.

For the nonlinear analysis the AAVSO magnitude data first need to be converted into a sequence with equal time-spacings, $\{s(t_n)\}$. We do this by performing 3 day averages that are then cubic-spline smoothed and interpolated with a σ=0.065. For comparison we will also show results with a 5 day average, and with smoothing parameters of σ=0.06 and σ=0.07. The reason for smoothing with a σ that is less than the observational noise (σ =0.15 mag, cf Fig. 1) is that we have already averaged the data which has introduced some smoothing. The observational data have many gaps, many of which are too large to bridge. We have therefore limited ourselves to the time-interval JD2445000 + 4400 days which has only three gaps (cf. Fig. 5, top).

Essentially all nonlinear analyses start with the construction of 'delay vectors' $\mathbf{X}(t_n) \equiv \mathbf{X}_n = \{s(t_n), s(t_n-\Delta), s(t_n-2\Delta), \ldots, s(t_n-(d_E-1)\Delta)\}$, where Δ is the 'delay' and d_E is the dimension of the 'reconstruction space'. The $\mathbf{X}_n$ provide a strobed representation of the 'trajectory' of the system in this d_E–dim space.

We now make the a priori assumption that the lightcurve is generated by a deterministic nonlinear mechanism of low dimension. Phrased differently, we assume that there is an operator (dynamics) that evolves the trajectory in time, i.e. it connects neighboring points of the trajectory. A theorem guarantees that there is a smooth one-to-one correspondence between the trajectory in the reconstruction space and the trajectory in the real or physical phase space of the system. Importantly, this diffeomorphism preserves some of the important properties of the dynamics in this correspondence. It is therefore possible to extract information about the physical dynamics from the observational data of a single observed variable $s(t)$ (the magnitude here). All we need to do is determine the functional form of the autonomous (time-independent) flow $d\mathbf{Z}/dt$ = $\mathbf{G}(\mathbf{Z})$ that gives rise to this trajectory $Z(t)$, and the observations provide the 'strobed' values $\mathbf{Z}(t_n)$ = $\mathbf{X}_n$.

A priori we do not know what values to give to the delay Δ and the dimension d_E. The delay should be large enough so that the attractor is not squashed onto the diagonal, but sufficiently small so that a polynomial nonlinearity can describe the flow. When the dimension of the reconstruction space is too small the trajectory can have intersections and other singularities (that are not allowed in an honest phasespace). There is therefore generally a *minimum* value for d_E, called the embedding dimension, in which the trajectory can be resolved, i.e. it is devoid of intersections and cusps. Nothing can be gained from increasing d_E beyond this value, but one can and should check that the properties of the reconstructed map stay invariant in higher dimensions. We are of course interested in finding this minimum value because it provides an upper bound on the dimensional

Table 1. Lyapunov exponents and dimension

d_E	Δ	p	σ	λ_1	λ_3	λ_4	λ_5	d_L	
3	5	6	0.065	0.0033	–0.034			2.10	†
3	10	6	0.065	0.0045	–0.026			2.17	
3	13	6	0.065	0.0069	–0.030			2.23	
4	5	5	0.065	0.0073	–0.016	–0.054		2.46	
5	6	4	0.065	0.0045	–0.023	–0.025	–0.032	2.19	†
5	7	4	0.065	0.0075	–0.009	–0.025	–0.056	2.85	
3	13	6	0.060	0.0015	–0.029			2.05	
3	3	6	0.070	0.0021	–0.037			2.06	
3	6	6	0.070	0.0032	–0.024			2.13	
5	6	4	0.070	0.0043	–0.015	–0.025	–0.036	2.29	
3	5	6	0.065	0.0025	–0.017			2.14	*
3	10	6	0.065	0.0013	–0.021			2.06	*
3	13	6	0.065	0.0015	–0.013			2.21	*

Lyapunov exponents in d^{-1}

† shown in Fig. 5

* with 5 day instead of 'standard' 3 day averages of AAVSOdata

of the physical dynamics, $d < d_E$, that underlies the observed signal (SKB).

For the quantitative reconstruction we turn to the global flow reconstruction method (q.v. SKB). We can equivalently reconstruct either a flow **G** or a 'map' **F** that connects the neighboring points on the trajectory. In SKB and BKSM we found that generally it is somewhat easier to construct maps, and that is what we do here. Our goal is thus to search for the best global polynomial map **F**, such that $\mathbf{X}_{n+1} = \mathbf{F}(\mathbf{X}_n)$.

Once we have constructed a map **F** we can iterate it and produce 'synthetic' signals that can then be compared to the observed lightcurve data. Since both are chaotic signals it would be meaningless to compare them point by point. Instead they need to be compared for their overall properties (cf. SKB, BKSM).

In Fig. 5, rows 2 and 3, we show two of the best synthetic signals that we have been able to construct in 3D and in 5D, respectively. The first has the parameters Δ= 5, p= 6, σ=0.065, d_E= 3, the second, Δ= 6, p= 4, σ=0.065, d_E= 5. (An earlier synthetic signal was already shown in a review by Buchler, Kolláth & Serre (1995) where first return maps were also presented). The synthetic signals reproduce the data reasonably well, although they are definitely somewhat 'tamer' than the latter.

Broomhead-King projections which are projections on the eigenvectors of the correlation matrix (q.v. SKB) provide a means to visualize the signals that is optimal in many ways. Thus in Fig. 6 we display the lowest Broomhead-King (BK) projections for the smoothed AC Her data in Col. 1. From the top down we display successively the projections ξ_2 vs. ξ_1, ξ_3 vs. ξ_1, ξ_3 vs. ξ_2. Col. 2 shows the 8–harmonic periodic signal that has been used to prewhiten the data earlier on (Fig. 2). This periodic signal clearly represents an average of the data. The BK projections of our best synthetic signals in 3D and 5D that have been shown in Fig. 5 are displayed in Cols. 3 and 6, respectively. The signal of Col. 7 will be discussed below.

We need to pause to say a word about what we mean by 'successful' or 'best' reconstructions. The synthetic signals that we reconstruct with a map are generally of two types, viz. are *limit cycles*, sometimes with period two, period 4, etc., or *chaos*. We hardly ever encounter fixed point attractors or multi-periodic ones (these latter could have 2 or 3 frequencies at most, i.e. 2 or 3–tori , since we have kept $d_E \leq 6$ in our analysis). Thus, the delay Δ=3 gives a limit cycle (omitted from Fig. 6), whereas with Δ=4 we get a 2-cycle (Col. 4 in Fig. 6), with Δ=5 a 4-cycle (Col. 5) and with Δ=6 a chaotic attractor (Col. 6). We note that the period two or four cycles that precede chaos when a parameter, such as Δ in the preceding example, is varied generally indicate that the structure of the map is close to what it takes to give chaos. Instead of being detrimental to our conclusion such period doubling cascades provide an indirect confirmation of the presence of nearby chaos.

We have summarized some of the tests in Table 1. The columns denote successively the reconstruction dimension d_E, the delay Δ, the highest order p of the monomials used in the map, and the smoothing parameter in the cubic spline fit to the AAVSO data. Next are shown the Lyapunov exponents of the synthetic signals λ_k, ordered with decreasing magnitudes. The last column contains the fractal Lyapunov dimension d_L that is an overall measure of the chaos. It is defined as (Ott 1993)

$$d_L = K + \sum_{j=1}^{K} \lambda_j / |\lambda_{K+1}| \,, \qquad (1)$$

with K the largest integer value for which the sum is positive.

The synthetic signals have reasonably robust properties as we go from d_E = 3 to the higher reconstruction dimension d_E =5. However, for a reason not understood it is a hard to get good maps in d_E=4. For some parameter values (e.g. entries 4 and 6 in Table 1) the reconstructions appear out of line with neighboring ones, with small values of $|\lambda_3|$ and concomitant large d_L (Eq. 1). For R Sct such egregious values were fewer, and we address probable causes in the next section. We just note here that short data sets with small signal to noise ratios are less than ideal for this nonlinear analysis, and that one would expect the results to get worse with increasing d_E because of the decrease in density (SKB, BKSM).

Table 1 also shows that the properties are also reasonably independent of the 'massaging', i.e. averaging, smoothing and interpolating of the observational data.

We draw attention to the following features:

(1) As expected all the $\lambda_1 > 0$, which constitutes a clear indication of chaos.

(2) Next, all $\lambda_2 \approx 0$ which, because of the high sampling rate, corroborates that an autonomous flow underlies the pulsations (cf. SKB).

(3) We are able to construct a good map in a reconstruction space as low as d_E=3, suggesting that the minimum embedding dimension is 3. However, we cannot rule out that we avoid all intersections and cusps in 3D (cf. SKB).

(4) It is very comforting that the successful reconstructions are stable in the sense that they give comparable properties in higher

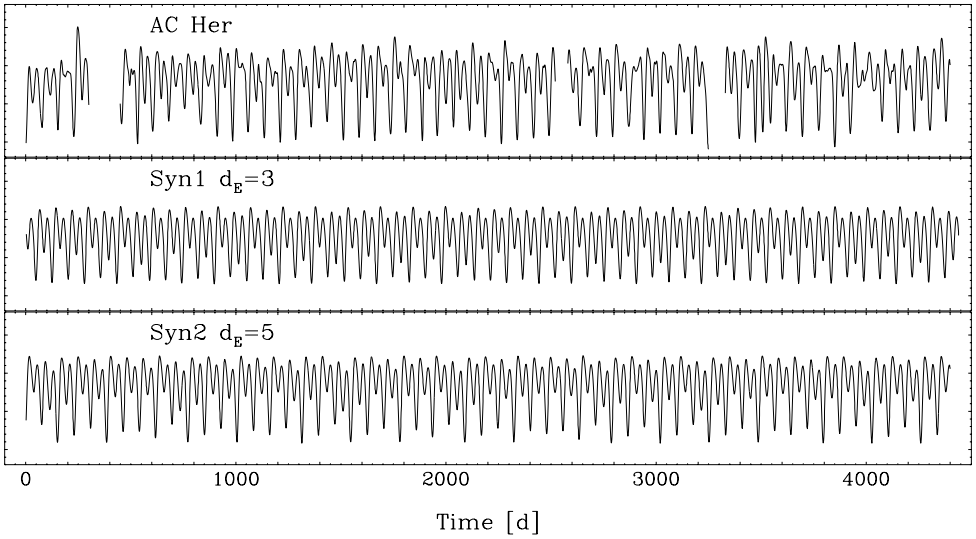

Fig. 5. Lightcurves; *Top*: AC Her, smoothed data (JD 2,445,000 + 4400 d); *Middle:* synthetic data (d_E=3, Δ=5, p=6, σ=0.065). *Bottom:* section of synthetic data from reconstructed global map (d_E=5, Δ=6, p=4, σ=0.065).

d_E as Table 1 shows.
(5) Except for unfortunate parameter combinations we find that $2.05 \lesssim d_L \lesssim 2.45$ for AC Her. Very importantly, the fractal dimension d_L is always well below 3, even for d_E = 5, and even in the worst reconstructions.

We do not display the FS of the synthetic signals, but note that whenever the Lyapunov dimension is in the range 2.05 – 2.2 the spectra compare rather well with the observed spectrum, Fig. 2. The less successful reconstructions, which also yield a higher d_L are shown in the Table, give a FS in which the first peak is very broadened. For this reason we believe that the d_L=2.45 just above provides a very generous upper limit.

Many spurious detections of chaos have been made in the literature, especially when techniques such as correlation dimensions are used, and one should therefore always be wary of such pitfalls. We therefore recall that SKB and BKSM did some tests that concluded that it is difficult to fool the global flow reconstruction method into erroneously predicting low-dimensional chaos on a stochastic signal.

As a test for the stability of the reconstruction for AC Her we have performed the following two experiments:

The first one is to take a section of our best chaotic synthetic signal (shown in Fig. 5 (row 3) and Fig. 6 (Col. 6) of the same length and sampled as the AAVSO data set, add Gaussian noise with the observational intensity of 0.15 mag, perform a 3 day averaging and a cubic spline smoothing with σ=0.065. The BK projections of this artificial signal are shown in col. 7 of Fig. 6, and they look very much like AC Her. When this signal is then subjected to the global flow reconstruction, interestingly, the reconstructed synthetic signal is again chaotic. Its Lyapunov dimension is found to be $d_L \approx 2.2$ for d_e = 3 and 2.4 for d_e = 5, i.e. in the broad range of the values for the AC Her lightcurve. It is quite reassuring that this second processing of the signal still yields chaos with properties similar to the first one.

The second test signal is taken to be stochastic. Starting with the periodic, 8 harmonic signal used to prewhiten the AC Her data in Fig. 2a, we added noise with the observational intensity of 0.15 mag. It is gratifying that just as in BKSM, only limit cycles are found. *No erroneous chaotic synthetic signals* are produced by the reconstruction for any of the values of d_E, Δ, p, σ that we have tried.

4. Discussion

In Sect. 2 we showed that it would be very difficult to interpret the lightcurve of AC Her as that of a steady periodic or multiperiodic star, or with that of a multiperiodic and evolving one. The next simplest working hypothesis is that the lightcurve is chaotic, i.e. that it is generated by a low dimensional dynamics with chaotic trajectories. In Sect. 3 we showed that indeed we can explicitly construct low dimensional flows with simple polynomial nonlinearities with properties close to the observed AC Her lightcurve.

We find that the reconstruction of maps is less robust for AC Her than it is for R Sct (BKSM). We see several reasons for this.
(a) First, the errors of the smoothed lightcurves are different: The individual measurement errors are somewhat larger for R Sct, 0.20 vs. 0.15 for AC Her. However the averaging process, $\approx$ 25 points/5 day vs. $\approx$ 5 points/3 day for AC Her causes the AC Her errors to be about a factor of 2 larger. A further factor of 2 comes from the smaller pulsation amplitude of AC Her, so that at the end, the errors of the smoothed lightcurve of R Sct are about a factor of 4 smaller than the corresponding AC Her. The reconstruction method therefore has greater difficulty in reconstructing the attractor from this noisier lightcurve data.
(b) The AC Her pulsations are more regular, and the trajectory explores a smaller region of phase space. Especially there is a complete absence of trajectories in the vicinity of the unstable fixed point of the map (or flow). This also has the drawback of determining less well the linear part of the map and the properties of the fixed point; In BKSM we linearized the map and could show that its unstable fixed point has 2 spiral roots, one unstable

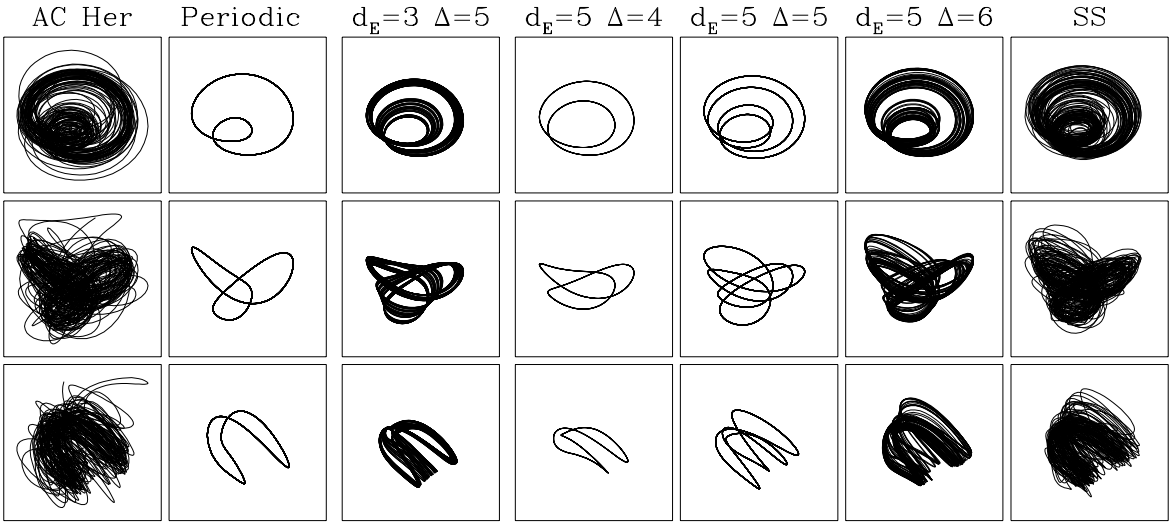

Fig. 6. Broomhead-King projections, from top down: (ξ_2 vs ξ_1), (ξ_3 vs ξ_1), (ξ_3 vs ξ_2); *Col. 1:* smoothed AC Her lightcurve; *Col. 2:* Periodic fit (8 harmonics) to the data; *Col. 3:* Synthetic signal for d_E=3, Δ=5. *Cols. 4–6:* Synthetic signals for delay vectors,d_E=5, Δ=4 through 6; *Col. 7:* Synthethic signal of col. 5 (Δ=6) with added noise, then sampled, averaged and smoothed like the AC Her data (see text);

and one stable with the trajectory running away from the fixed point with the fundamental frequency to return later toward the fixed point with approximately twice this frequency. This was interpreted as showing that the chaotic behavior of R Sct is the result of the nonlinear interaction of two vibrational modes that are in an approximate 2:1 resonance. A similar argument is thus not possible here.

(c) The more irregular features in the observational data are too few to have a sufficient influence on the map construction, e.g. the peak near 220 d and the 'unusual' oscillation near 3500 d. These features are also prominent as the few very large excursions in the BK plots of the first column of Fig. 6. When these wildest excursions are disregarded the AC Her projections and the Δ=6 reconstructions become quite similar. This is quite apparent in the noisy smoother synthetic signal of Col. 7 of Fig. 6 that has already been discussed.

We note though that whenever the synthetic solutions resemble the observational data and have a similar Fourier spectrum, they have similar Lyapunov exponents and low Lyapunov dimension, this independently of reconstruction dimension d_E. Most importantly, the Lyapunov dimension d_L is always considerably less than 3, independently of the dimension of the reconstruction space d_E. The fact that we can get maps with good synthetic signals in 3 dimensions already suggests that the embedding dimension is perhaps as low as d_E = 3.

From the inequality $d_L < d \leq d_E$, and the values d_e =3 and $2.05 \lesssim d_L \lesssim 2.45 < 3$ that we have determined we conclude (cf. SKB) that the physical Euclidean dimension of the underlying attractor is probably as low as 3.

When the results of our analysis of AC Her are compared with those of R Sct, on the one hand, and with the pulsations of W Vir models one notices a trend, which is already obvious from a visual inspection of he lightcurves: As the period increases the alternations in the shallow and deep minima as well as the modulations become increasingly irregular. This behavior is also observed in a quantitative fashion in the Lyapunov dimension that increases from $\approx$ 2.05 for the W Vir model, to $\approx$ 2.05–2.45 for AC Her and to $\approx$ 3.1 for R Sct. It appears that one may therefore be able to extract useful quantitative information from irregular lightcurves. In turn, that this will put novel and very useful constraints on the numerical modelling of these objects. On the theoretical side a thorough numerical hydrodynamical survey of W Vir and RV Tau models is clearly also necessary to confirm this hope.

5. Conclusions

AC Her is the second irregular variable star that we have analyzed with the global flow reconstruction method. Our conclusion is that the pulsations of AC Her are most likely the result of low dimensional chaos. However, because of the inferior quality of the observational data the case is not quite as strong as for R Sct for which we have little doubt as to the chaotic nature of the pulsations. We also recall in support of this conclusion that the numerical hydrodynamical modelling of the pulsations of W Vir type stars (KB88 and Serre, Kolláth & Buchler 1995b) showed very clearly low dimensional chaos.

We finish with a plea for observational data on RV Tau stars. The available observational data are far from optimal for nonlinear analyses. We stress that good continuous coverage (typically some 20 points per cycle) are necessary, but that, contrary to Fourier analysis, even long gaps do not pose a problem for nonlinear analyses.

Acknowledgements. This research has been supported in part by NSF (AST92-18068, AST95-28338, INT94-15868), a Hungarian OTKA grant (F4352), an RDA grant at UF, the French Ministère pour la Recherche et l'Espace, and RCI grant from IBM through UF.

References

Abarbanel, H. D. I., Brown, R., Sidorowich, J. J., Tsimring, L. S. 1993, Rev. Mod. Phys. 65, 1331

Buchler, J. R., 1997, Int'l School of Phys. "Enrico Fermi", Course CXXXIII on *"Past and Present Variability of the Solar-Terrestrial System: Measurement, Data Analysis and Theoretical Models"*, Eds. G. Cini Castagnoli & A. Provenzale (in press).

Buchler, J.R. 1993, in *Nonlinear Phenomena in Stellar Variability*, p. 9, Eds. M. Takeuti & J.R. Buchler, Dordrecht: Kluwer Publishers, reprinted from 1993, Ap&SS, 210

Buchler, J. R., Serre, T., Kolláth, Z. & Mattei, J. 1995, Phys. Rev. Lett. 74, 842 [BSKM]

Buchler, J. R., Kolláth, Z. Serre, T., 1995, in *Waves in Astrophysics*, Eds. J.H. Hunter & R.E. Wilson, Ann. NY Acad. Sci. 773, p. 1

Buchler J. R., Kolláth, Z., Serre, T. & Mattei, J. 1996, ApJ 462, 489 [BKSM]

Gouesbet, G., LeSceller, L, Letellier, C., Brown, R., Buchler, J.R. & Kolláth, Z. 1997, *Nonlinear Signal and Image Processing*, Ann. N.Y. Acad. Sci. Vol. 808, p. 25.

Kovács, G. & Buchler, J. R. 1988, ApJ, 334, 971, [KB88].

Ott, E. 1993, *Chaos in Dynamical Systems* (Univ. Press: Cambridge)

Percy, J.R., Bezuhly, M. Milanowski, M. & Zsoldos, E. 1997. PASP 109, 264

Percy, J.R. & Mattei, J.A. 1993. Ap&SS 210, 137 PASP 109, 264

Serre, T., Kolláth, Z. & Buchler, J. R. 1995a, A&A 311, 833 [SKB]

Serre, T., Kolláth, Z. & Buchler, J. R. 1995b, A&A 311, 845

Weigend, A. S. & Gershenfeld, N. A. 1994, *Time Series Prediction* (Reading: Addison-Wesley)

Zsoldos, E. 1988, IBVS, 3192

This article was processed by the author using Springer-Verlag LaTeX A&A style file *L-AA* version 3.